

# Radiative Weak Annihilation Decays

Richard F. Lebed

*Jefferson Lab, 12000 Jefferson Avenue, Newport News, VA 23606*

(August, 1999)

## Abstract

A class of meson decay modes sensitive to only one quark topology at leading  $G_F$  order (annihilation of valence quarks through a  $W$ ) is described. No experimental observations, nor even upper limits, have been reported for these decays. This work presents a simple-minded (order-of-magnitude) calculation of their branching fractions, and compares to results of previous calculations where available. Although rare, one of these modes ( $D_s^+ \rightarrow \rho^+\gamma$ ) might already be observable at charm experiments, two others ( $D^+ \rightarrow K^{*+}\gamma$ ,  $B^+ \rightarrow D_s^{*+}\gamma$ ) should appear at the  $B$  factories, and the rest at hadron colliders.

13.25.Ft, 13.40.Hq, 13.25.Jx

## I. INTRODUCTION AND MOTIVATION

As data on charm and beauty decays accumulates at CLEO, BES, and the Fermilab and LEP experiments, and soon at the  $B$  factories BABAR and BELLE, it becomes possible to study ever more rare decays in search of interesting and exotic physics. This work suggests examining a largely overlooked class, electromagnetic decays of a charged meson mediated by the weak annihilation of the meson. Such decays are indeed rare, with branching ratios (BRs) suppressed by  $\alpha$ , not to mention the difficulty of forcing a camel (the whole meson wavefunction) through the eye of a needle (the pointlike  $W$  vertex multiplied by CKM factors), but their BRs need not be so tiny as one might think.

Let us focus upon processes with only one meson in the final state. Such decays are especially interesting because they proceed through only one weak decay topology at leading order in  $G_F$  if *i*) the flavors of all the valence quarks in both initial and final states are distinct, and *ii*) the initial and final quark have the same electric charge (and similarly for the antiquarks). This is the  $s$ -channel annihilation topology presented in Fig. 1. Note that the first condition requires each valence quark to terminate on a flavor-changing vertex, while the second eliminates the possibility of a  $t$ -channel  $W$  exchange. The photon may be attached to any charged line, although of course couplings to the lighter constituents are favored. At  $O(G_F^2)$  corrections enter through diagrams with a penguin loop on each of the quark and antiquark lines (Fig. 2*a*), crossed-box diagrams (Fig. 2*b*), and the diagram with the photon coupled to the  $W$ , none of which is expected to be very large. In addition, one may go beyond the valence diagrams and describe the weak process including its short-distance QCD corrections in terms of operators mixed through evolution of the corresponding anomalous dimension matrix,<sup>1</sup> but we do not perform this refinement in this work.

The interest in such decays lies partly in the simplicity of the weak topology and sensitivity to a number of hard-to-isolate CKM elements (as well as strong and electromagnetic matrix elements), and partly in the simplicity of the two-body final state. Indeed, the hard, monochromatic final-state photon should prove an exceptionally unambiguous experimental signal for these decays. It should also be pointed out that these modes would represent the first electromagnetic decays observed for the charged  $0^-$  mesons  $D^+$ ,  $D_s^+$ ,  $B^+$  (except for the famous penguin mode  $B^+ \rightarrow K^{*+}\gamma$ ), or  $B_c^+$ . Table I presents decays representing the 6 possible weak annihilation flavor assignments obeying our constraints, along with the CKM factors in the amplitude and their behavior in powers of the Wolfenstein parameter  $\lambda \approx 0.22$ .

To our knowledge, the Cabibbo-unsuppressed mode  $D_s^+ \rightarrow \rho^+\gamma$  was first studied in Ref. [3] via quark model, then through pole and vector meson dominance (VMD) calculations [4], light-cone [5], and effective field theory techniques [6]. Estimates for  $\text{BR} \times 10^5$  vary from 2.1 [3] to 80 [6] (see Ref. [7] for a summary). The present calculation, which for simplicity only takes into account one pole diagram in the language of Refs. [4,6], gives  $8 \times 10^{-5}$ . The double Cabibbo-suppressed mode  $D^+ \rightarrow K^{*+}\gamma$  was also studied in Refs. [4,6], with BR results ranging from  $3\text{--}30 \times 10^{-7}$ ; we obtain  $6 \times 10^{-7}$ . Encouraged by this consistency

---

<sup>1</sup>Here we refer to mixing of the usual four-fermi operator with its Fierz reordering. One finds [1,2] that the coefficient of the original operator can be enhanced by 20% or more.

with the more elaborate calculations, we apply our simple picture to the  $B^+$  and  $B_c^+$  modes. While  $D_s^+ \rightarrow \rho^+\gamma$  is exciting because it might already appear in charm experiment data,  $D^+ \rightarrow K^{*+}\gamma$  is interesting because it exhibits a neturinoless decay sensitive to  $|V_{cs}|$ .

The modes  $B^+ \rightarrow D_s^{*+}\gamma$  and  $D^{*+}\gamma$  (collectively,  $D_{(s)}^{*+}\gamma$ ), were suggested [8] as probes of  $|V_{ub}|$  and were estimated to have BRs of approximately  $2 \times 10^{-7}$  and  $7 \times 10^{-9}$ , respectively. From Table I we see that the  $B^+$  decays suffer the worst CKM suppressions. A number of the theoretical uncertainties associated with these estimates can be eliminated if the on-shell photon is replaced by an  $\ell^+\ell^-$  pair [9], and the invariant mass  $q^2$  of the virtual photon is used to define an operator product expansion. The price one pays for this improvement is an extra factor of  $\alpha$ , so that such decays are estimated to have BRs of a few times  $10^{-10}$  or  $10^{-12}$ , depending upon the level of Cabibbo suppression. The  $t$ -channel exchange processes mentioned above, which have neutral initial- and final-state mesons, are discussed in Ref. [10], and yield similar BRs. Most of these processes are too rare to be seen in appreciable numbers at the  $B$  factories (with combined yields of some millions of  $B^+B^-$  pairs per year [11]), but may be observable at hadron collider experiments.

The  $B_c$  modes appear to have been studied only using the light-cone approach, in Ref. [2]. We obtain BR results several orders of magnitude larger than theirs, and comment on this discrepancy below.

The rest of this paper is organized as follows: In Sec. II, we present a very simple-minded calculation of the rate for these processes and a list of approximations used, while Sec. III presents numerical results, outlines experimental prospects for the observation of these modes, lists potential theoretical improvements, and concludes.

## II. CALCULATION

The calculation presented in this section is very simplistic, in that it relies on a number of substantial approximations made explicit below. However, it is significant not in providing an exact determination of widths and BRs, but in obtaining the order of magnitude of these quantities as an estimate for experimenters searching for signals of these modes, and as a point of comparison for theorists performing subsequent, more refined calculations.

The generic process we consider is  $M \rightarrow P \rightarrow V\gamma$ , where  $M$  is the massive initial  $0^-$  state,  $P$  is a lighter virtual  $0^-$  meson with the flavor quantum numbers of the final state, and  $V$  is the final-state  $1^-$  meson, as depicted in Fig. 3. For the charm decays, we have commented that consistency with the more elaborate calculations in Refs. [4,6] indicates that this elementary ansatz seems to capture the essential order-of-magnitude physics. This approach avoids the danger of large cancellations between competing diagrams, but also runs the risk of missing important contributions in some cases. In modeling the decay this way, we make the following assumptions:

1. Photon emission from  $M$  is neglected, so the process  $M \rightarrow M^*\gamma \rightarrow V\gamma$  is not included, as was done in Refs. [4,6,8]. Indeed, the  $D_{(s)}D_{(s)}^*\gamma$  couplings have only measured upper bounds. In the charm case, Refs. [4,6] used  $D_{(s)}D_{(s)}^*\gamma$  input from previous theoretical calculations. In Ref. [8], where  $M = B^+$ ,  $M^* = B^{*+}$ ,  $P = D_{(s)}^+$ , and  $V = D_{(s)}^{*+}$ , the  $MM^*\gamma$  and  $PV\gamma$  couplings were related through heavy quark spin-flavor symmetry (HQS) to that of  $DD^*\gamma$ , and both diagrams were included. However, in the current

case with, for example,  $V = K^{*+}$  or  $\rho^+$ , this is no longer an acceptable approximation, and we include only the photon coupling to the lighter mesons. This assumption likely leads to an underestimate of the BR, but probably not an exceptionally large one: The  $K^{*+}$  and  $\rho^+$  electromagnetic widths are  $50 \pm 5$  and  $68 \pm 7$  keV, respectively, while that of the  $D^{*+}$  is less than 4.2 keV;<sup>2</sup> moreover, the calculations of Refs. [4,6] show the  $D_{(s)}D_{(s)}^*\gamma$  amplitudes to be about 1/4 as large as those for  $PV\gamma$ . Conversely, the light-cone calculations [2,5] include only the photon coupling to  $M$ , arguing that couplings to  $V$  are suppressed by light quark masses.

2. Complete factorization with vacuum insertion approximation is assumed for the weak vertex. The annihilation of  $M$  and the creation of  $P$  are assumed to occur at a single point. This approximation neglects both the short-distance QCD corrections as mentioned above, and long-distance hadronic contributions. As an example of the latter, the initial weak vertex may, rather than annihilating the initial meson, produce a quark (or antiquark)  $q$  that is the antiparticle of one of the meson valence quarks, and this four-quark intermediate state propagates for some time before  $q\bar{q}$  annihilation occurs. Specifically, processes like  $D^+ \rightarrow (K^+\pi^0 \text{ or } K^0\pi^+) \rightarrow K^{*+}\gamma$ , which require an understanding of final-state interactions, are not included, nor are the significant VMD diagrams such as  $D^+ \rightarrow K^{*+}\rho^0 \rightarrow K^{*+}\gamma$ , where the  $\rho$  couples resonantly to a photon; nevertheless, the CKM coefficient of all these diagrams is the same.
3. The intermediate state  $P$  is assumed to be the lightest pseudoscalar with the same flavor quantum numbers as the final-state  $V$ . Certainly many other resonant as well as multiparticle states with total angular momentum 0 (that of  $M$ ) can couple the weak vertex to  $V\gamma$ ; however, the parity-violating couplings to  $0^+$  states are neglected here. The present assumption is made partly because data exists on the  $PV\gamma$  coupling from the observed decay  $V \rightarrow P\gamma$ , and partly because the lightest pseudoscalar  $P$  among all possible intermediates presumably has the one of the largest couplings to  $V\gamma$  due to a relatively large wavefunction overlap. In any case, this approximation leads to an underestimate of the correct BR.
4. In comparing the virtual process  $P \rightarrow V\gamma$  to the on-shell  $V \rightarrow P\gamma$ , one relates the single (magnetic) form factor  $\mathcal{C}(q^2)$  at a virtuality of  $q^2 = m_M^2 - m_P^2$  to that at  $q^2 = 0$ . We take them numerically equal, although this tends to overestimate the rate, since form factors tend to fall off away from  $q^2 = 0$ . Nevertheless, we indicate this ratio explicitly in the final expression, see Eq. (2.4) below.

Given these assumptions, the calculation of the rate is a simple matter. The weak mixing vertex, mediated by an operator  $\mathcal{O}_W$ , in vacuum insertion approximation is given by

$$\begin{aligned} & \langle P(p_M) | \mathcal{O}_W | M(p_M) \rangle \\ &= -i \frac{G_F}{\sqrt{2}} V_P V_M B \langle P(p_M) | \bar{Q}_P \gamma^\mu (1 - \gamma_5) q_P | 0 \rangle \langle 0 | \bar{q}_M \gamma_\mu (1 - \gamma_5) Q_M | M(p_M) \rangle \end{aligned}$$

---

<sup>2</sup>Nonetheless, one should note that a small propagator denominator ( $m_V^2 - m_{M^*}^2$ ) or different a light quark charge in  $M^*$  can enhance the importance of such couplings in the full width.

$$\begin{aligned}
&= -i \frac{G_F}{\sqrt{2}} V_P V_M B \left( -i f_P p_M^\mu \right) \left( +i f_M \bar{p}_{M\mu} \right) \\
&= -i \frac{G_F}{\sqrt{2}} V_P V_M f_P f_M M^2 B,
\end{aligned} \tag{2.1}$$

where  $m_M$  is now abbreviated as  $M$ , the valence structure of  $P$  is  $Q_P \bar{q}_P$ , that of  $M$  is  $Q_M \bar{q}_M$ , and  $V_{M,P}$  are the CKM parameters associated with the annihilation of  $M$  and creation of  $P$ , respectively. We also allow for a coefficient  $B$  parameterizing the incompleteness of the vacuum saturation approximation, as in  $\bar{B}B$  mixing, but set it to unity in our numerical estimates. The intermediate  $0^-$  state  $P$  provides the simple propagator  $i/(p_M^2 - m_P^2)$ . The photon vertex is extracted from the decay  $\Gamma_{V \rightarrow P\gamma}$ , which has invariant amplitude

$$\mathcal{M} = \mathcal{C}(p_P^2 - m_P^2) \epsilon_{\mu\nu\rho\sigma} \epsilon_V^\mu \epsilon_\gamma^{*\nu} p_\gamma^\rho p_V^\sigma, \tag{2.2}$$

where the Lorentz coupling is determined in part by the  $0^-$  quantum number of  $P$ .  $\mathcal{C}$  is a magnetic form factor, and simply becomes a transition magnetic moment when its momentum transfer argument  $p_P^2 - m_P^2$  is set to zero in the on-shell case. The rate obtained from this amplitude is

$$\Gamma_{V \rightarrow P\gamma} = \frac{1}{12\pi} \mathcal{C}^2(0) E_\gamma^3. \tag{2.3}$$

The full rate for  $M \rightarrow V\gamma$  also uses  $\mathcal{C}^2$ , but now has the argument  $M^2 - m_P^2$ . For our numerical estimates, we assume that  $\mathcal{C}$  does not change dramatically over this range, and use data on  $\Gamma_{V \rightarrow P\gamma}$  to eliminate  $\mathcal{C}$  from the expression for  $\Gamma_{M \rightarrow V\gamma}$ ; however, since this is certainly a contentious approximation, we formally retain the ratio of  $\mathcal{C}$  at the two different argument values in the full expression for the width. Putting this together, one obtains our central result:

$$\begin{aligned}
\Gamma(M \rightarrow V\gamma) &= \frac{3}{2} G_F^2 |V_M V_P|^2 f_M^2 f_P^2 B^2 \Gamma_{V \rightarrow P\gamma} \left[ \frac{\mathcal{C}(M^2 - m_P^2)}{\mathcal{C}(0)} \right]^2 \\
&\times \left( \frac{M^2}{M^2 - m_P^2} \right)^2 \left( \frac{M^2 - m_V^2}{m_V^2 - m_P^2} \right)^3 \left( \frac{m_V}{M} \right)^3.
\end{aligned} \tag{2.4}$$

Here, the cubed mass factors are nothing more than the ratio of  $E_\gamma^3$  for  $M \rightarrow V\gamma$  to that for  $V \rightarrow P\gamma$ .

One may compare Eq. (2.4) to Eq. (17) of Ref. [8] for  $B^+ \rightarrow D_{(s)}^{*+}$ , which in the current notation reads

$$\begin{aligned}
\Gamma(M \rightarrow V\gamma) &= \frac{27}{8} G_F^2 |V_M V_P|^2 f_M^4 B^2 \Gamma_{V' \rightarrow P'\gamma} \left[ \frac{\mathcal{C}(M^2 - m_P^2)}{\mathcal{C}(0)} \right]^2 \\
&\times \left[ \frac{m_V M (M - m_V) (M + m_V)^3}{(m_{V'}^2 - m_{P'}^2)^3} \right] \left( \frac{m_{V'}}{M} \right)^3,
\end{aligned} \tag{2.5}$$

where the  $0^-, 1^-$  pair  $P', V'$  are related to  $P, V$  by HQS: The primed mesons are introduced when data for  $\Gamma_{V \rightarrow P\gamma}$  is unavailable. In Ref. [8],  $P', V'$  were  $D^+, D^{*+}$  and the experimental upper bounds for  $D^{*+} \rightarrow D^+\gamma$  were used; the current calculation uses only information

from the unprimed mesons directly, so  $P', V' \rightarrow P, V$  here. All of the differences between Eqs. (2.4) and (2.5) can be accounted for by the assumptions of HQS: First, the magnetic moment form factors for all heavy mesons were assumed the same, except for a trivial coefficient due to the electric charge  $Q_{q(m)}$  of the lighter quark  $q$  in the meson  $m$  to which the photon couples. Since both the  $MM^*\gamma$  and  $PV\gamma$  couplings were included in the HQS calculation, an extra enhancement of  $(Q_{q(M)} + Q_{q(V)})^2/Q_{q(V)}^2$ , a factor of 9, appeared in Ref [8]. Next, in HQS one has  $f_M^2 M = f_P^2 m_P$ , and  $m_V - m_P = O(1/M)$ ,  $M$  being the heavy quark mass. The remaining differences arise from the fact that fields containing heavy quarks in HQS are nearly static, even if the heavy quark changes flavor. This leads one to adopt the normalization of HQS states of 1 rather than  $2M$  particles per unit volume, as well as introduce propagators linear rather than quadratic in particle masses, and these modifications often lead to effective lowest-order substitutions (in the current notation) such as  $(M + m_V)/2 \rightarrow M$ . Equations (2.4) and (2.5) are related by the application of these properties.

### III. RESULTS AND CONCLUSIONS

We employ Eq. (2.4) to obtain BR estimates for the 6 modes exhibited in Table I. We use standard *Review of Particle Physics* (RPP) [12] values for masses, decay constants, CKM elements, and lifetimes whenever possible, with the following exceptions: We take  $|V_{ub}| = 3 \times 10^{-3}$ ,  $f_B = 170$  MeV, and  $f_D = f_{D_s} = 200$  MeV. Following recent experiments, we use the E791 value [13]  $\tau_{D_s} = 0.518 \pm 0.014 \pm 0.007$  psec, and the CDF values [14]  $m_{B_c^+} = 6.40 \pm 0.39 \pm 0.13$  GeV,  $\tau_{B_c^+} = 0.46_{-0.16}^{+0.18} \pm 0.03$  psec. OPAL [15] and ALEPH [16] have also reported a few  $B_c$  candidate events, with mass values consistent with Ref. [14]. We also use the most recent lattice determinations [17] of  $f_{B_c}$ , which combined give  $425 \pm 11$  MeV. As mentioned previously, we take  $B^2 = 1$  and  $\mathcal{C}^2(M^2 - m_P^2)/\mathcal{C}^2(0) = 1$ .

The resulting BRs are exhibited in Table II, along with the energies of the final-state photon. We see that the  $B^+$  modes give BRs in agreement with Ref. [8], despite a very different calculation, and similarly for the  $D_{(s)}^+$  decays in comparison with Refs. [3–6], as promised in Sec. I. A few  $D^+ \rightarrow K^{*+}\gamma$  and  $B^+ \rightarrow D_s^{*+}\gamma$  should appear each year at the  $B$  factories, with the exact number depending upon the correct value of the mantissa in our estimate. The mode  $D_s^+ \rightarrow \rho^+\gamma$  might even be observable right now at charm experiments such as at BES (or possibly CLEO) if our estimate is low by a factor of a few, or the upper bounds of the estimates in Refs. [4,6] are correct, based on limits in the RPP [12]; in any case, existing experiments can place a meaningful upper limit on its BR.

However, in contrast to Ref. [2], we find that the  $B_c^+$  modes are rare but not exceptionally so; they find  $\text{BR}(B_c \rightarrow \rho^+\gamma) = 8.3 \times 10^{-8}$  and  $\text{BR}(B_c \rightarrow K^{*+}\gamma) = 5.3 \times 10^{-9}$ . This  $O(10^3)$  discrepancy might be explainable if  $\mathcal{C}(0)/\mathcal{C}(m_B^2 - m_\pi^2) \approx 30$ , but then the order-of-magnitude agreement for  $D_{(s)}$  and  $B$  decays becomes a mystery. Furthermore, even if the form factor  $\mathcal{C}$  falls off this dramatically, other longer-distance mechanisms (see point 2 in Sec. II) would likely step in to maintain the rate. Of course, since the  $B$  factories are not designed to produce  $B_c$ 's, the possible observation of these modes must necessarily wait for the upcoming hadron collider experiments at the LHC or Tevatron.

Although much physics is neglected in this simple calculation, our estimates show that weak annihilation decays may be observed in the near future. They are attractive from both

the experimental and theoretical perspective. Improvement of the theoretical calculation essentially amounts to improving on the four assumptions made in Sec. II. Lifting the first requires new data for the heavy coupling in  $M^* \rightarrow M\gamma$ , particularly positive data for  $D^{*+} \rightarrow D^+\gamma$ . Improving the vacuum insertion approximation can be accomplished as in  $\bar{B}B$  mixing, with lattice or model calculations, and including the short-distance QCD corrections is a straightforward matter. Many of the neglected long-distance corrections such as VMD diagrams have been considered in Refs. [4,6], but one must take care with their relative phases, while final-state interactions must still be taken into account. As for the remaining two assumptions, one can be freed of both the lowest-resonance dominance and constant form factor assumptions by either including other intermediate channels explicitly, or carrying out light-cone or inclusive quark model calculations.

From the experimental side, it would be interesting to see what direct bounds can be placed on these modes at the current time, in anticipation of their eventual observation. Once observed, the weak annihilation modes will present an interesting probe of CKM elements, electromagnetic transitions, and meson wavefunctions.

### Acknowledgments

I thank C. Carlson, C. Carone, A. Petrov, and V. Sharma for useful discussions, and G. Burdman and S. Prelovšek for pointing out important references. This work is supported by the Department of Energy under contract No. DE-AC05-84ER40150.

## REFERENCES

- [1] M. Bauer, B. Stech, and M. Wirbel, *Z. Phys. C* **34**, 103 (1987).
- [2] T. M. Aliev and M. Savci, *J. Phys. G* **24**, 2223 (1998).
- [3] P. Asthana and A. N. Kamal, *Phys. Rev. D* **43**, 278 (1991).
- [4] G. Burdman, E. Golowich, J. L. Hewett, and S. Pakvasa, *Phys. Rev. D* **52**, 6383 (1995).
- [5] A. Khodjamirian, G. Stoll, and D. Wyler, *Phys. Lett. B* **358**, 129 (1995).
- [6] S. Fajfer, S. Prelovšek, and P. Singer, *Eur. Phys. J. C* **6**, 471 (1999); S. Fajfer and P. Singer, *Phys. Rev. D* **56**, 4302 (1997); B. Bajc, S. Fajfer, and R. J. Oakes, *Phys. Rev. D* **51**, 2230 (1995).
- [7] S. Fajfer, S. Prelovšek, and P. Singer in Ref. [6], Table 2.
- [8] B. Grinstein and R. F. Lebed, *Phys. Rev. D* **60**, 031302(R) (1999).
- [9] D. H. Evans, B. Grinstein, D. R. Nolte, *Phys. Rev. D* **60**, 057301 (1999); Report No. UCSD/PTH 99-05, hep-ph/9904434 (unpublished).
- [10] D. H. Evans, B. Grinstein, D. R. Nolte, Report No. UCSD/PTH 99-05, hep-ph/9906528 (unpublished).
- [11] See, for example, *The BABAR Physics Book*, P. F. Harrison and H. R. Quinn, editors, Report No. SLAC-R-504, Stanford Linear Accelerator, Stanford, CA, 1998.
- [12] Particle Data Group (C. Caso *et al.*, *Review of Particle Physics*, *Eur. Phys. J. C* **3**, 1 (1998).
- [13] E791 Collaboration (E. M. Aitala *et al.*), *Phys. Lett. B* **445**, 449 (1999).
- [14] CDF Collaboration (F. Abe *et al.*), *Phys. Rev. Lett.* **81**, 2432 (1998).
- [15] OPAL Collaboration (K. Ackerstaff *et al.*), *Phys. Lett. B* **420**, 157 (1998).
- [16] ALEPH Collaboration (R. Barate *et al.*), *Phys. Lett. B* **402**, 213 (1997).
- [17] B. D. Jones and R. M. Woloshyn, *Phys. Rev. D* **60**, 014502 (1999); C. T. H. Davies *et al.*, *Phys. Lett. B* **382**, 131 (1996).

TABLES

Valence structure	Decay mode	CKM Elements
$\bar{b}u \rightarrow c\bar{s}\gamma$	$B^+ \rightarrow D_s^{*+}\gamma$	$V_{ub}^*V_{cs} \sim \lambda^3$
$\bar{b}u \rightarrow c\bar{d}\gamma$	$B^+ \rightarrow D^{*+}\gamma$	$V_{ub}^*V_{cd} \sim \lambda^4$
$\bar{b}c \rightarrow u\bar{s}\gamma$	$B_c^+ \rightarrow K^{*+}\gamma$	$V_{cb}^*V_{us} \sim \lambda^3$
$\bar{b}c \rightarrow d\bar{u}\gamma$	$B_c^+ \rightarrow \rho^+\gamma$	$V_{cb}^*V_{ud} \sim \lambda^2$
$c\bar{d} \rightarrow u\bar{s}\gamma$	$D^+ \rightarrow K^{*+}\gamma$	$V_{cd}^*V_{us} \sim \lambda^2$
$c\bar{s} \rightarrow u\bar{d}\gamma$	$D_s^+ \rightarrow \rho^+\gamma$	$V_{cs}^*V_{ud} \sim \lambda^0$

TABLE I. Flavor structure and mesonic decay modes of weak annihilation electromagnetic decays. The CKM coefficient for each process is accompanied by its magnitude in powers of Wolfenstein  $\lambda \approx 0.2$ .

Decay mode	BR (est.)	Photon Energy (GeV)
$B^+ \rightarrow D_s^{*+}\gamma$	$1 \times 10^{-7}$	2.22
$B^+ \rightarrow D^{*+}\gamma$	$7 \times 10^{-9}$	2.26
$B_c^+ \rightarrow K^{*+}\gamma$	$3 \times 10^{-6}$	3.14
$B_c^+ \rightarrow \rho^+\gamma$	$3 \times 10^{-5}$	3.15
$D^+ \rightarrow K^{*+}\gamma$	$6 \times 10^{-7}$	0.72
$D_s^+ \rightarrow \rho^+\gamma$	$8 \times 10^{-5}$	0.83

TABLE II. Estimates of branching ratios for weak annihilation decays using Eq. (2.4). Also included are energies of the monochromatic photon.

FIGURES

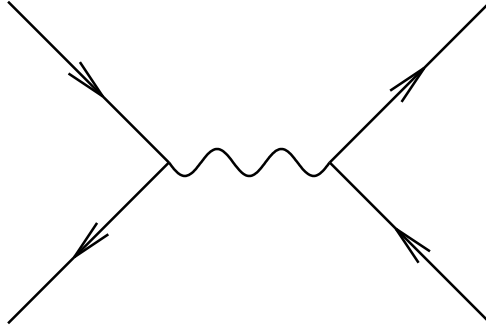


FIG. 1. The  $s$ -channel weak annihilation topology.

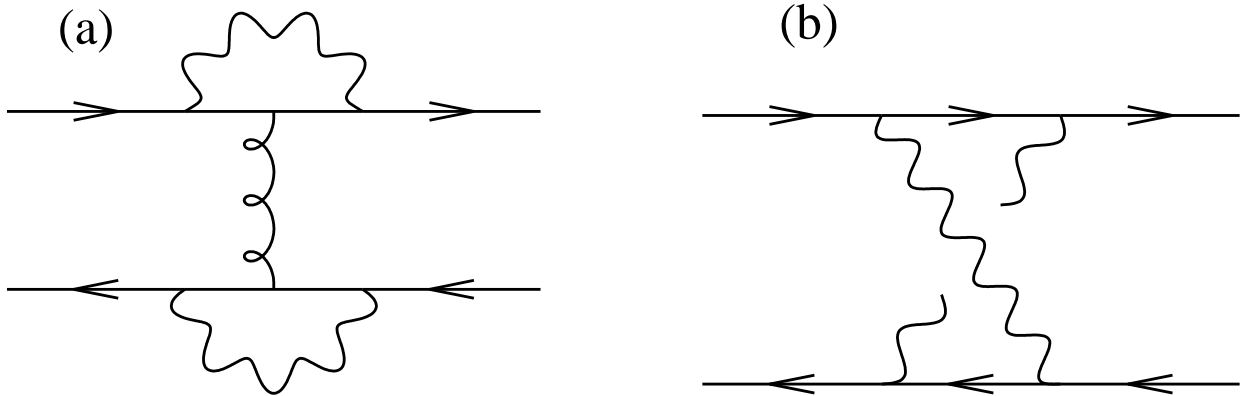


FIG. 2.  $O(G_F^2)$  corrections to Fig. 1: (a) di-penguin diagram; (b) crossed-box diagram.

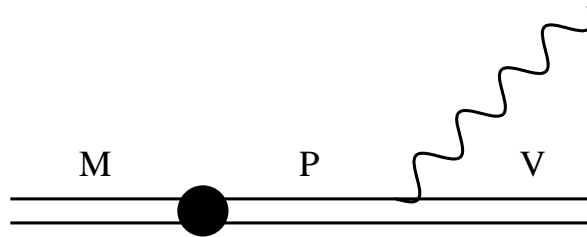


FIG. 3. Meson decay diagram for the process  $M \rightarrow P \rightarrow V\gamma$ . The blob represents the flavor-changing vertex of Fig. 1 and its corrections.